PROGRESS IN ENGINEERING APPLICATION AND TECHNOLOGY
e-ISSN: 2773-5303

PEAT

Vol. 5 No. 2 (2024) p. 178-187
https://publisher.uthm.edu.my/periodicals/index.php/peat

Fault Classification in GCPV Microgrid System Using Wavelet Transform

Mohamad Hakimi Zullkuffli[1], Faridah Hanim Mohd Nor[1]*

[1] *Department Of Electrical Engineering Technology, Faculty Of Engineering Technology, University Tun Hussein Onn Malaysia, Pagoh, 84600, Muar Johor, MALAYSIA*

*Corresponding Author: hanim@uthm.edu.my
DOI: https://doi.org/10.30880/peat.2024.05.02.018

Article Info

Received: 27 June 2024
Accepted: 17 July 2024
Available online: 25 November 2024

Keywords

Grid-connected photovoltaic (GCPV) microgrids, Maximum power extraction, Fault detection, Wavelet transform techniques, 3-phase voltage analysis, Solar PV array voltage, Fault classification and identification.

Abstract

Grid-connected photovoltaic (GCPV) microgrids have emerged as a promising alternative to conventional energy sources. To ensure efficient operation, maximum power needs to be extracted from the PV system and the 3-phase grid system. PV panels are often connected in series and parallel combinations, forming an array to meet load demands. However, the system can experience various faults, such as grid faults, PV system faults, and grid faults with the PV system in normal conditions. These faults can lead to significant reductions in maximum power generation and affect the load. In this project, MATLAB SIMULINK was used to simulate the circuit with wavelet transform techniques. Wavelet transform techniques are employed to detect damage events by analysing the 3-phase voltage and solar PV array voltage. Wavelet decomposition using 'wavedec' and detailed coefficient extraction using 'detcoef' enable fault classification and identification. The wavelet coefficients can identify all faults, allowing for early isolation of damage locations. By using this method, 15 fault conditions were identified in 4 locations: 2 locations in the PV system and 2 locations in the grid system.

1. Introduction

A microgrid is a localized system of electricity generation and distribution that can operate either connected to or separated from the existing power grid, combining various distributed power sources such as solar photovoltaic (GCPV) systems, energy storage, and cogeneration to supply the electricity required by local users, with the main advantage being increased reliability of electricity supply through simultaneous generation from multiple sources; however, GCPV systems are susceptible to faults causing voltage and current transients and discontinuities that adversely affect power quality, and conventional protection methods are insufficient for accurately detecting and localizing such faults in microgrids with high penetration of inverter-based resources, necessitating the use of more advanced signal processing techniques like wavelet transforms which have shown promise for accurately capturing the transient edges of faults, though open challenges remain regarding real-time hardware implementation, optimal choice of wavelet basis functions, and coordination with existing protection elements, requiring further research to develop adaptive wavelet-based protection schemes that can reliably detect, classify, and locate faults under varying operating conditions in GCPV microgrids with rigorous testing across diverse fault and disturbance scenarios, as the development of such robust integrated grid protection solutions will be key to enabling the wider deployment of GCPV microgrids and realizing their full potential benefits[1][2]; therefore, the objectives of this project are to develop a wavelet transform-based fault protection method in GCPV microgrid systems and evaluate its effectiveness through simulations using MATLAB Simulink, investigating the capability of the microgrid in both grid-connected and islanded modes of operation, as well as in

This is an open access article under the CC BY-NC-SA 4.0 license.

looped and radial configurations, with parameters for the PV system including 2 parallel strings with 10 series modules, each operating at 60V, and the grid voltage being 415V rms, which corresponds to 200-220V per phase, and the proposed approach has shown promising results and can be used as a reliable and efficient method for fault protection in microgrids.

Various methods have been proposed for fault protection and detection in microgrids. One approach involves using wavelet multiresolution analysis to preprocess voltage and current signals for computing total harmonic distortion [3]. Another focuses on identifying fault locations in double-circuit transmission lines using discrete wavelet transform compared to Fast Fourier Transform [4]. A different method integrates Sequential Overlapping Differential Transform to detect faults in AC microgrids by forming characteristic frequency bands from zero-mode current transient components [5]. For DC microgrids, recurrent neural networks (RNNs) combined with decision tree classifiers are utilized for fault detection and location using feeder current and main bus voltage inputs [6]. Additionally, an artificial neural network (ANN) is employed to diagnose and isolate faults in DC microgrid systems preemptively [7].

2. Method

This chapter focuses on the method used in this project, which utilizes wavelet transform. This simulation was conducted using coding and MATLAB software, where the software utilizes 20GB of RAM to run this simulation smoothly with the main library being Simscape Electrical. The fault classification method employed for navigation uses wavelet transform.

2.1 Process of GCPV Microgrid System

Figure 1 shows the block diagram. The GCPV Microgrid system included PV Array, MPPT, DC-DC Converter, Energy Storage, Control Unit and Load.

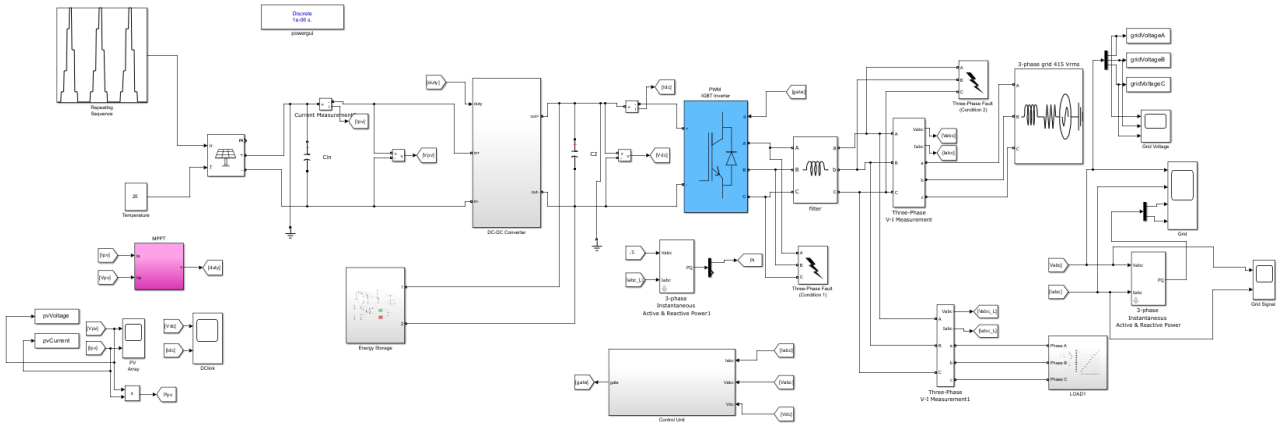

Fig 1 *GCPV Microgrid System*

Meanwhile, Figure 2 describes a block diagram of the process for the GCPV Microgrid System to be carried out. The process starts with an array of photovoltaic panels that harness energy from sunlight and generate direct current (DC) electricity. This DC power then goes through a Maximum Power Point Tracking algorithm (MPPT) that continuously adjusts the electrical load on the PV array to extract the maximum available power. The optimized DC electricity from the MPPT is then fed to a DC-to-DC converter which steps up the voltage to appropriately charge the battery storage. The battery storage acts as an energy reservoir, accumulating power when the sun is shining for use at night or during cloudy weather when the PV array cannot generate electricity. The stored DC power from the batteries is inverted into alternating current (AC) electricity using Pulse Width Modulation (PWM) Insulated Gate Bipolar Transistor (IGBT) inverter. This AC conversion is required since household devices and the utility grid operate on AC power. The inverter's AC output is filtered to obtain a clean sine wave before being supplied to electrical loads or interfaced with the 3-phase grid. Any additional power needed, or excess power generated can be dynamically fed from or to the grid to maintain balance in the system. Finally, the system uses 3-phase Voltage-Current (V-I) measurement to measure voltage and current, and 3-phase Instantaneous Active & Reactive Power Calculation component to determine the real and reactive power being generated or consumed. These measurements allow for monitoring and control of the photovoltaic system's performance.

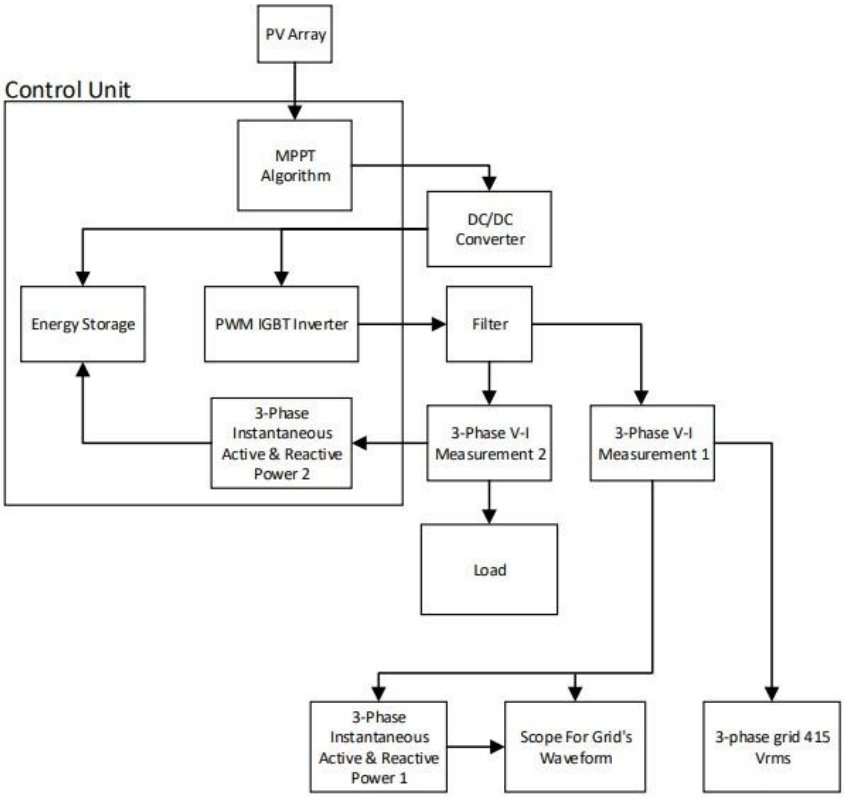

Fig 2 Flowchart GCPV Microgrid System

2.2 System Flowchart

In this system, the flowchart shows the process starting with the use of wavelet transform to identify the maximum coefficient in each phase. After obtaining the values of the maximum coefficients, fault classification techniques are applied using MATLAB SIMULINK coding to identify 15 fault conditions.

2.2.1 Wavelet Transform

The flowchart on figure 3 shows a 3-level wavelet decomposition process for analysing signals. It starts with the input signal which first goes through a high pass filter and a low pass filter. The high pass filter extracts the high frequency components while the low pass filter extracts the low frequency components. The output of the low pass filter (A1) contains the low frequency trend of the signal. A1 then goes through down sampling by 2, which reduces the sampling rate by half. Down sampling prepares the signal for the next level of decomposition.

In the second level, A1 goes through the same process again. It is split by a high pass and low pass filter into high frequency parts (D2) and low frequency parts (A2). The low frequency A2 is down sampled by 2 again. This repeats similarly for the third level - A2 is filtered into D3 (high frequency) and A3 (low frequency), with A3 being down sampled. The outputs D1, D2 and D3 represent the fine detailed coefficients of the signal at different resolutions. A3 represents the general overall trend and approximation of the signal. This multi-level filtering and down sampling allows wavelet analysis to examine a signal at different scales and resolutions. It enables multi-resolution signal processing for compression, noise removal, feature extraction and more.

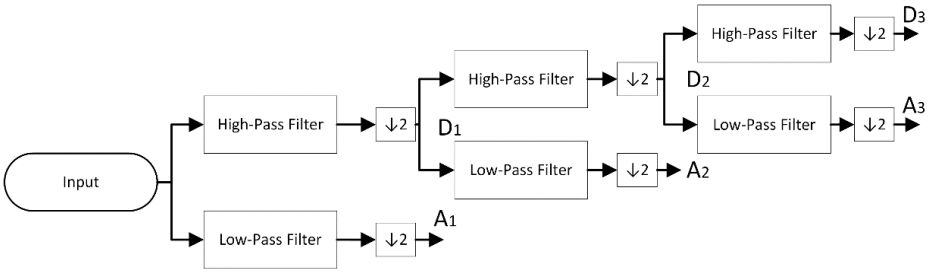

Fig 3 Wavelet Structure

Progress in Engineering Application and Technology Vol. 5 No. 2 (2024) p. 178-187

Next, is applying wavelet transform. First step is to decompose the signal using the wavedec function. This function performs a multi-level 1-D wavelet decomposition. The 'wavedec' function decomposes the input signal 'x' into approximation and detail coefficients at multiple levels. Meanwhile the output 'c' is a concatenated vector of all the coefficients, and 'l' is a vector indicating the number of coefficients at each level. Below is the syntax of "wavedec".

[c, l] = wavedec(x, n, wname);

x : The input signal that you want to decompose.
n : The number of decomposition levels (wavelet layers). If not specified, the default is 1.
wname : The name of the wavelet to use for the decomposition (e.g., 'haar', 'db1' for Daubechies, etc.).
c : The output wavelet decomposition vector, which contains the wavelet coefficients.
l : A vector that contains the number of coefficients by level.

Second step is extracting the detailed coefficients at a specific level using the detcoef function. The 'detcoef' function extracts the detailed coefficients from the decomposition vector 'c' at the specified level 'n'. These detailed coefficients represent the high-frequency components of the signal at that level. Below is the syntax of "detcoef".

D = detcoef(c, l, n);

c : The wavelet decomposition vector obtained from wavedec.

l : The vector containing the number of coefficients by level.

n : The specific decomposition level from which you want to extract the detailed coefficients.

D : The detailed coefficients at the specified level.

2.2.2 Fault Classification Technique

Figure 4 shows a process for detecting and identifying faults in a three-phase electrical power system. The process starts with the "Start" symbol, indicating the start of the procedure. The first step is "Run Simulation", where the Simulink model `gridconnectedpvinvertersuccesspreviousvers.slx` is executed. Following this, this flowchart branches into two in parallel namely "Grid Fault Detection" and "PV Fault Detection". In the "Grid Fault Detection" step, the wavelet decomposition of the grid voltage for phases A, B and C is performed and the maximum values of the detail coefficients (`m`, `n` and `p`) are extracted. At the same time, in the "PV Fault Detection" step, the wavelet decomposition of the PV voltage is carried out, and the maximum value of the detail coefficient (`z`) is determined.

Next, the flowchart focuses on the "Display Debug Values" step, where the `m`, `n`, `p` and `z` values are displayed for debugging purposes. These values will then be determined in the "Fault Detection Logic" decision, where these values will determine specific conditions to determine the type of damage found in the system. The decision node branches into multiple paths based on the values of `m`, `n`, `p` and `z`, leading to different damage detection results. These results include detecting various types of faults such as Three Phase Fault Detected at Location 1, PV System Fault at location 1 (FC1), Grid in Normal Condition, PV System has Fault at Location 1 (FC2), Three Phase Fault Detected at Location 2, PV System Fault at location 1 (FC3), Three Phase Fault Detected at Location 1, PV System Fault at location 2 (FC4), Grid in Normal Condition, PV System has Fault at Location 2 (FC5), Three Phase Fault Detected at Location 2, PV System Fault at location 2 (FC6), Three Phase Fault Detected at Location 1 and Location 2, PV System Fault at location 1 (FC7), Three Phase Fault Detected at Location 1 and Location 2, PV System Fault at location 2 (FC8), Three Phase Fault Detected at Location 1 and Location 2, PV System Fault at location 1 and location 2 (FC9), Grid in Normal Condition, PV System has Fault at Location 1 and Location 2 (FC10), Three Phase Fault Detected at Location 1, PV System in Normal Condition (FC11), Grid in Normal Condition, PV System in Normal Condition, (FC12), Three Phase Fault Detected at Location 2, PV System in Normal Condition (FC13), Three Phase Fault Detected at location 1 and Location 2, PV System in Normal Condition (FC14).

Finally, the process ends with a "Done" symbol, indicating the completion of the error detection procedure. This flowchart provides a clear and structured approach to fault identification in grid-connected PV inverter systems by analyzing grid and PV voltages using wavelet decomposition and evaluating specific conditions.

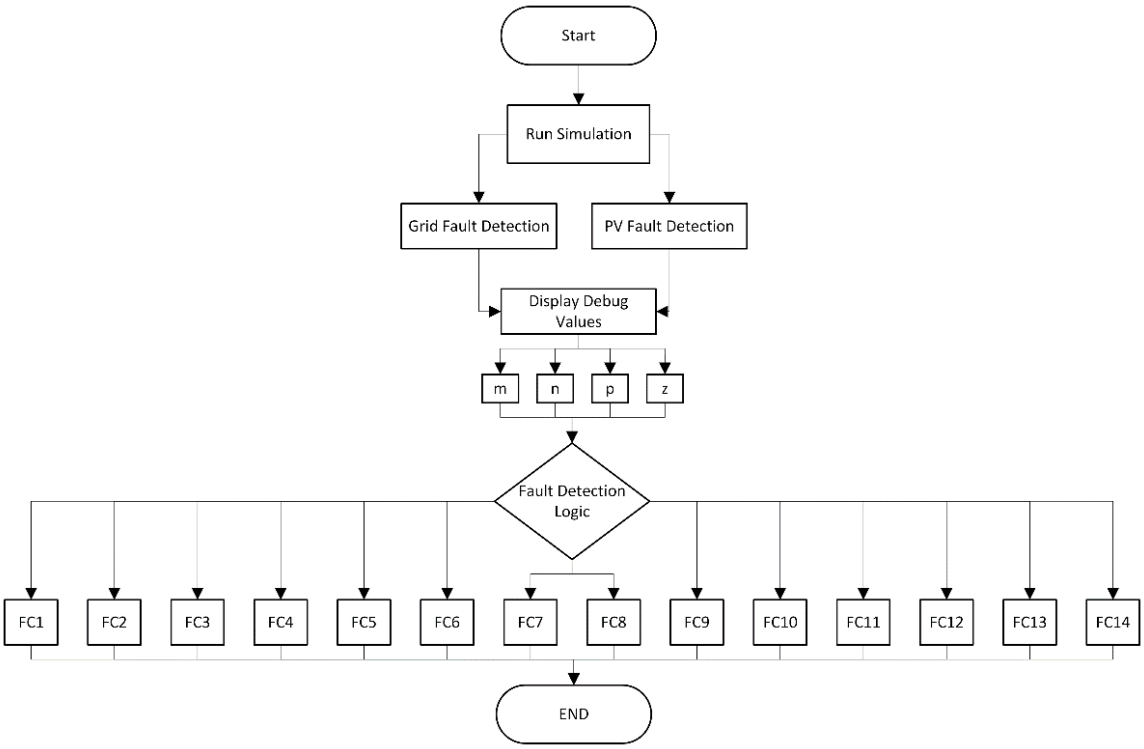

Fig 4 Fault Classification Technique

3. Result

The results show that faults occurred in 4 locations which is 2 locations in the 3-phase grid at 415 Vrms and 2 locations in the PV system. The output results indicate 15 fault conditions occurring across these 4 locations.

3.1 Location of Fault

Figure 5 shows the location of the fault has been determined. There are several locations where faults occur in the PV system and the 3-phase grid (415 Vrms), each with 15 possible fault conditions and 1 unknown condition. Figure 5 below illustrates the locations of these faults. The first and second locations represent faults that occurred in the PV system that is in a grounded short circuit, which will cause the circuit to fail. Meanwhile, the third and fourth locations represent faults that occurred in the 3-phase grid (415 Vrms).

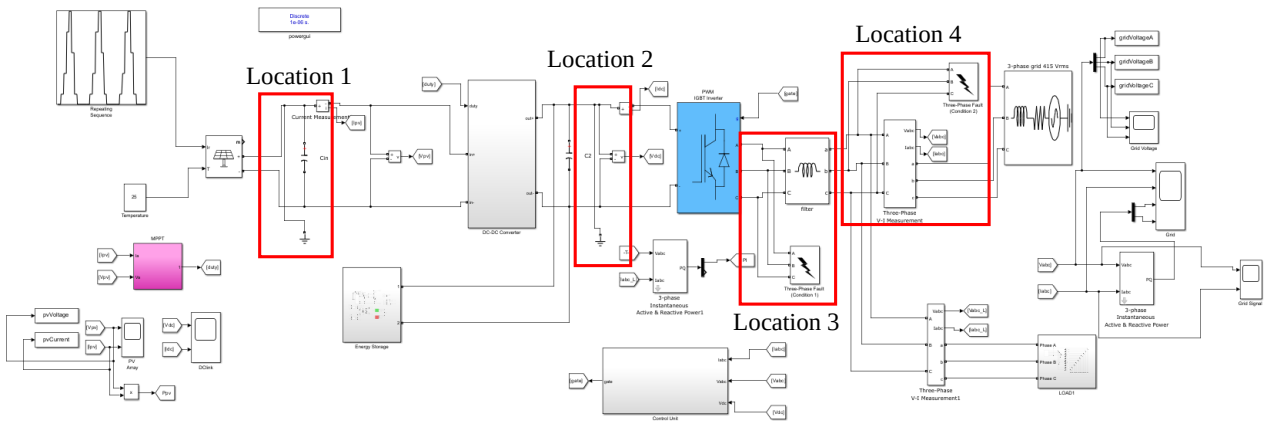

Fig 5 Location of Fault

Progress in Engineering Application and Technology Vol. 5 No. 2 (2024) p. 178-187

3.2 Maximum Coefficient on Grid and on PV System

There are 15 fault conditions. The maximum coefficient values have been determined using wavelet decomposition with the syntax 'wavedec' and subsequently extracting detailed coefficients using the syntax 'detcoef'. Table 1 below shows the results of the maximum coefficients for all fault types.

Table 1 The Maximum Coefficient on 3-phase grid (415 Vrms) and on PV System

No	Fault type	Max Coefficient of Phase A (V)	Max Coefficient of Phase B (V)	Max Coefficient of Phase C (V)	Max Coefficient of Phase Z (V)
1	Three Phase Fault Detected at Location 1, PV System Fault at location 1	9.9404	60.0602	29.3763	0.91037
2	Grid in Normal Condition, PV System has Fault at Location 1	3.9011	59.493	29.3763	0.061235
3	Three Phase Fault Detected at Location 2, PV System Fault at location 1	7.626	59.8011	66.2634	0.031941
4	Three Phase Fault Detected at Location 1, PV System Fault at location 2	15.1774	74.7567	29.3763	0.00022932
5	Grid in Normal Condition, PV System has Fault at Location 2	7.5556	74.8876	29.3763	0.00022744
6	Three Phase Fault Detected at Location 2, PV System Fault at location 2	7.7236	74.8775	66.8415	0.00024517
7	Three Phase Fault Detected at Location 1 and Location 2, PV System Fault at location 1	5.958	60.043	66.2987	0.87688
8	Three Phase Fault Detected at Location 1 and Location 2, PV System Fault at location 2	7.4586	74.7789	66.8427	0.00024511
9	Three Phase Fault Detected at Location 1 and Location 2, PV System Fault at location 1 and location 2	6.2381	70.9261	68.9979	0.29696
10	Grid in Normal Condition, PV System has Fault at Location 1 and Location 2	4.6408	70.858	29.3763	0.27422
11	Three Phase Fault Detected at Location 1, PV System in Normal Condition	36.816	58.9678	46.9709	0.000064436
12	Grid in Normal Condition, PV System in Normal Condition	2.6922	59.5172	29.3771	0.000064436
13	Three Phase Fault Detected at Location 2, PV System in Normal Condition	18.5957	60.0281	68.5607	0.00012353
14	Three Phase Fault Detected at location 1 and Location 2, PV System in Normal Condition	9.9569	61.4195	68.5608	0.000064436
15	Uknown Condition	7.9202	49.45	29.3763	0.00068755

The table provides data on various fault conditions in a 3-phase grid and PV system, including the maximum coefficients of phases A, B, C, and Z for different scenarios. In the 3-phase grid, there are phases A, B, and C, while in the PV system, there is phase Z. The scenarios include three-phase faults at locations 1 and 2, and PV system faults at locations 1 and 2. The coefficients show the data in the 3-phase grid, specifically in phases A, B, and C. During fault conditions, the values are more than 2.6922V for phase A, between 58.976V and 74.8876V for phase B, and between 29.3763V and 68.9979V for phase C. Meanwhile, in the PV system, when a fault occurs, the value of the coefficients is more than 0.000064436V. In normal conditions, the value of the coefficients in the 3-phase grid must be 2.6922V for phase A, 59.5172V for phase B, and 29.3771V for phase C, and in the PV system, it must be 0.000064436V. When there is a new fault location, the coefficient data will show 7.9202V for phase A, 49.45V for phase B, 29.3763V for phase C, and 0.00068755V for phase Z.

3.3 Output at Command Window

Table 2 below shows the output on every probability of fault happened in 3-phase grid system and PV system.

Table 2 Output of All Type of Fault

No	Fault type	Output
1	Three Phase Fault Detected at Location 1, PV System Fault at location 1	Command Window m: 9.9404 n: 60.0602 p: 29.3763 z: 0.91037 Three Phase Fault Detected at Location 1, PV System Fault at location 1
2	Grid in Normal Condition, PV System has Fault at Location 1	Command Window m: 3.9011 n: 59.493 p: 29.3763 z: 0.061235 Grid in Normal Condition, PV System has Fault at Location 1
3	Three Phase Fault Detected at Location 2, PV System Fault at location 1	Command Window m: 7.626 n: 59.8011 p: 66.2634 z: 0.031941 Three Phase Fault Detected at Location 2, PV System Fault at location 1
4	Three Phase Fault Detected at Location 1, PV System Fault at location 2	Command Window m: 15.1774 n: 74.7567 p: 29.3763 z: 0.00022932 Three Phase Fault Detected at Location 1, PV System Fault at location 2
5	Grid in Normal Condition, PV System has Fault at Location 2	Command Window m: 7.5556 n: 74.8876 p: 29.3763 z: 0.00022744 Grid in Normal Condition, PV System has Fault at Location 2
6	Three Phase Fault Detected at Location 2, PV System Fault at location 2	Command Window m: 7.7236 n: 74.8775 p: 66.8415 z: 0.00024517 Three Phase Fault Detected at Location 2, PV System Fault at location 2
7	Three Phase Fault Detected at Location 1 and Location 2, PV System Fault at location 1	Command Window m: 5.958 n: 60.043 p: 66.2987 z: 0.87688 Three Phase Fault Detected at Location 1 and Location 2, PV System Fault at location 1

Progress in Engineering Application and Technology Vol. 5 No. 2 (2024) p. 178-187

8	Three Phase Fault Detected at Location 1 and Location 2, PV System Fault at location 2	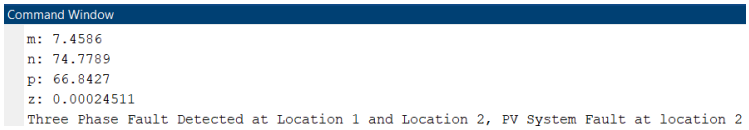
9	Three Phase Fault Detected at Location 1 and Location 2, PV System Fault at location 1 and location 2	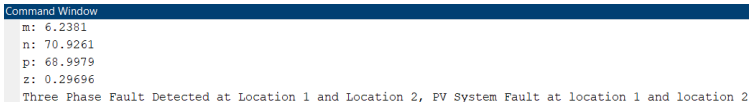
10	Grid in Normal Condition, PV System has Fault at Location 1 and Location 2	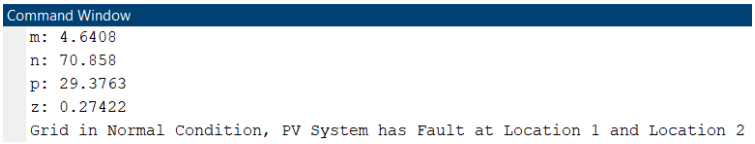
11	Three Phase Fault Detected at Location 1, PV System in Normal Condition	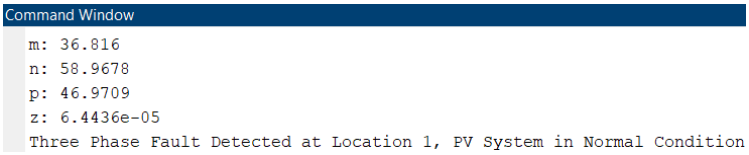
12	Grid in Normal Condition, PV System in Normal Condition	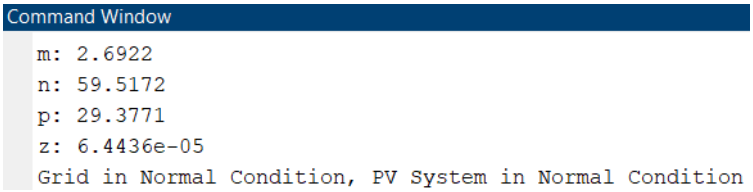
13	Three Phase Fault Detected at Location 2, PV System in Normal Condition	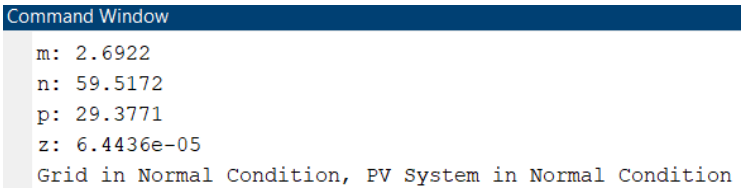
14	Three Phase Fault Detected at location 1 and Location 2, PV System in Normal Condition	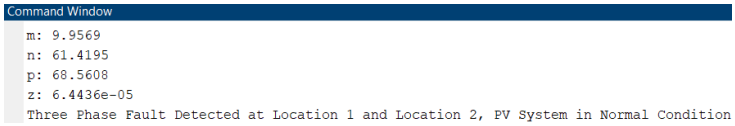
15	Uknown Condition	

3.4 Summary

In conclusion, the data for each maximum coefficient on every phase is very important as it will determine the condition of the fault. All this data comprises 15 fault conditions and 1 unknown condition, which include faults occurring at the first and second locations in the PV system and the third and fourth locations in the 3-phase grid system. All this data will produce different outputs depending on the type of fault and the location where the fault happened. The efficiency of obtaining the best output is very high; however, it will decrease if the probability location of the fault changes or when new components are added.

4. Conclusion

Wavelet Transform (WT) is a popular method for detecting and classifying faults in power systems because it can analyze signals in both time and frequency domains. However, WT has some significant limitations. One of the main issues is that it relies heavily on threshold values to classify faults. These threshold values are not universal and need to be recalibrated for each new power system, which can be a tedious and time-consuming process. This recalibration is necessary to ensure that the system can accurately classify different types of faults under various conditions.

To overcome these limitations, several advanced techniques have been proposed. One promising approach is the use of Artificial Neural Networks (ANNs). ANNs can learn from data and generalize well to new situations. They can handle complex, non-linear relationships and are robust to noise, making them ideal for fault detection and classification in power systems. By training ANNs on pre-fault and post-fault voltage and current waveforms, they can accurately classify faults without needing predefined threshold values. In summary, while Wavelet Transform is a useful tool for fault detection and classification in power systems, its limitations require the use of more advanced techniques. Artificial Neural Networks offer robust solutions to enhance the accuracy, reliability, and generalizability of fault classification systems. By integrating these advanced methods, we can significantly improve power system protection, ensuring faster and more accurate fault detection and classification.

Acknowledgement

The author sincerely acknowledges the collaboration provided by Universiti Tun Hussein Onn Malaysia. Gratitude is also extended to all individuals, both directly and indirectly involved in the compilation of this thesis. The authors express appreciation to the Faculty of Engineering Technology, Universiti Tun Hussein Onn Malaysia, for their invaluable help, support, and insightful advice throughout this project. Their guidance was essential in developing concepts and ensuring the successful completion of the project. Their patience, inspiration, and unwavering support have been instrumental throughout this journey. Their belief in my abilities and constant encouragement empowered me to overcome challenges and remain focused.

References

[1] S. Pant, R. K. Nema, and S. Gupta, "Detecting Faults in Power Transformers Using Wavelet Transform," in *2021 IEEE 2nd International Conference on Electrical Power and Energy Systems, ICEPES 2021*, Institute of Electrical and Electronics Engineers Inc., 2021. doi: 10.1109/ICEPES52894.2021.9699483.

[2] Z. Li, "Wavelet Transform Based Methods for Fault Detection and Diagnosis of HVDC Transmission Systems Recommended Citation," 2019. [Online]. Available: https://dc.uwm.edu/etd/2094

[3] S. Baloch, S. S. Samsani, and M. S. Muhammad, "Fault Protection in Microgrid Using Wavelet Multiresolution Analysis and Data Mining," *IEEE Access*, vol. 9, pp. 86382–86391, 2021, doi: 10.1109/ACCESS.2021.3088900.

[4] A. H. Bin Mustapha *et al.*, "Fault location identification of double circuit transmission line using discrete wavelet transform," *Indonesian Journal of Electrical Engineering and Computer Science*, vol. 15, no. 3, pp. 1356–1365, Sep. 2019, doi: 10.11591/ijeecs.v15.i3.pp1356-1365.

[5] H. Huang, Z. Gong, H. Shu, and X. Tian, "Microgrid fault detection method based on sequential overlapping differential transform," in *2020 IEEE 4th Conference on Energy Internet and Energy System Integration: Connecting the Grids Towards a Low-Carbon High-Efficiency Energy System, EI2 2020*, Institute of Electrical and Electronics Engineers Inc., Oct. 2020, pp. 2308–2313. doi: 10.1109/EI250167.2020.9347290.

[6] A. A. Sharif, H. K. Karegar, and S. Esmaeilbeigi, "Fault Detection and Location in DC Microgrids by Recurrent Neural Networks and Decision Tree Classifier," in *2020 10th Smart Grid Conference, SGC 2020*, Institute of Electrical and Electronics Engineers Inc., Dec. 2020. doi: 10.1109/SGC52076.2020.9335743.

[7] I. Almutairy and M. Alluhaidan, "Fault Diagnosis Based Approach to Protecting DC Microgrid Using Machine Learning Technique," in *Procedia Computer Science*, Elsevier B.V., 2017, pp. 449–456. doi: 10.1016/j.procs.2017.09.019.

[8] A. A. Sharif, H. K. Karegar, and S. Esmaeilbeigi, "Fault Detection and Location in DC Microgrids by Recurrent Neural Networks and Decision Tree Classifier," in *2020 10th Smart Grid Conference, SGC 2020*, Institute of Electrical and Electronics Engineers Inc., Dec. 2020. doi: 10.1109/SGC52076.2020.9335743.

[9] *40th North American Power Symposium : September 28-September 30 2008, University of Calgary, Calgary, Alberta, Canada.* IEEE, 2008.

[10] J. Do Park, J. Candelaria, L. Ma, and K. Dunn, "DC ring-bus microgrid fault protection and identification of fault location," *IEEE Transactions on Power Delivery*, vol. 28, no. 4, pp. 2574–2584, 2013, doi: 10.1109/TPWRD.2013.2267750.